Charge-carrier injection characteristics at organic/organic heterojunction interfaces in organic light-emitting diodes

Toshinori Matsushima [a], Kenichi Goushi [b], and Chihaya Adachi [a, b, *]

[a] *Core Research for Evolutional Science and Technology Program (CREST), Japan Science and Technology Agency (JST), 1-32-12 Higashi, Shibuya, Tokyo 150-0011, Japan*

[b] *Center for Future Chemistry, Kyushu University, 744 Motooka, Nishi, Fukuoka 819-0395, Japan*

Organic light-emitting diodes (OLEDs) having various guest molecules doped in an organic host matrix layer are fabricated [the OLED structure is anode/hole-transporting layer (HTL)/guest-host emitting layer/hole-blocking layer/electron-transporting layer/cathode], and the dependence of current density-voltage (*J*-*V*) characteristics of the OLEDs on highest occupied molecular orbital (HOMO) levels of guest molecules are investigated. From the *J*-*V* characteristics of these OLEDs, we find two important results: (1) *J*-*V* characteristics of the OLEDs are controlled by the direct hole injection from the neighboring HTL to guest molecules, and (2) HOMO level alignment between the HTL and guest molecules provides efficient hole injection at this interface.

[*]Corresponding author. Tel and Fax: +81 92 802 3294

E-mail address: adachi@cstf.kyushu-u.ac.jp (C. Adachi)

Recently, energetic research on organic light-emitting diodes (OLEDs) is being conducted due to their high potentials for low-cost, wide-scale, lightweight, flexible display, and illumination applications. The key technique commonly used in high-performance OLEDs reported thus far is doping fluorescent or phosphorescent organic guest molecules in large energy-gap organic host matrixes [1-6]. This guest-host hybrid layer embedded in an OLED structure is crucial for enhancing electroluminescence efficiencies. In fact, multiplayer OLEDs having highly efficient phosphorescent iridium complexes doped in appropriate host matrixes can reach an internal EL quantum efficiency of nearly 100% [3-6]. However, current flow mechanisms of multilayer OLEDs are still underdeveloped and must be clarified to develop future organic optoelectronic devices. A detailed understanding of current flow mechanisms will provide a guide line for reducing driving voltages and improving long-term reliability, both of which are required for commercial display applications. Therefore, in this work, we investigated current flow mechanisms of multilayer OLEDs with various host-guest systems.

We fabricated OLEDs having various guest molecules doped in a large energy-gap 4-4´-bis(carbazol-9-yl)-2,2´-biphenyl (CBP) host matrix layer to investigate how their current density-voltage (*J*-*V*) characteristics depend on the highest occupied molecular

orbital (HOMO) levels of guest molecules. The device structure was glass substrate/indium tin oxide (ITO) anode/N,N´-di(m-tolyl)-N,N´-diphenylbenzidine (TPD) hole-transporting layer (HTL)/5 mol%-guest-doped CBP host matrix layer/2,9-dimethyl-4,7-diphenyl-1,10-phenanthroline (BCP) hole-blocking layer/tris-(8-hydroxyquinoline) aluminum (Alq_3) electron-transporting layer/MgAg cathode (see Fig. 1). This multilayer OLED structure is widely used to confine excitons in the CBP layer [7-9] and using the CBP host matrix can prevent concentration quenching of excitons on guest molecules, thereby providing efficient energy transfer from large energy-gap CBP to small energy-gap guest molecules. In these devices, electrons from the MgAg cathode are preferentially blocked at the TPD/CBP interface, and holes from the ITO anode are subsequently injected in the CBP layer, resulting in the recombination of electrons and holes. Here, we observed that this hole injection process at the TPD/CBP interfaces predominantly controlled the *J-V* characteristics of our devices. In particular, the device doped with an 2-phenyl-5-[4-(5-phenyl-2-thienyl)phenyl]thiophene (AC-5) guest molecule having a HOMO level of -5.3 eV exhibited the highest current density, while using guest molecules with HOMO levels other than -5.3 eV resulted in a gradual decrease in current density. Since this HOMO level of -5.3 eV is identical with that of the TPD HTL, we found that the

difference in energy (HOMO) levels between the TPD and guest molecules significantly affected hole injection efficiencies at this heterojunction interface.

The OLEDs doped with the various guest molecules were fabricated according to the following steps. Glass substrates coated with 100-nm-thick ITO layers were ultrasonically cleaned in detergent/water, followed by pure water, acetone, and isopropanol. Prior to vacuum preparations of organic layers, the substrates were placed in an ultraviolet-ozone treatment chamber. Then, 50-nm-thick TPD, 20-nm-thick CBP, 10-nm-thick BCP, and 30-nm-thick Alq_3 layers were successively evaporated in a vacuum on the cleaned ITO surface at an evaporation rate of 0.3 nm/s. During CBP evaporation, the doping concentration of the guest to CBP molecules was precisely controlled at 5 mol% using two separate quartz thickness monitors. Finally, a 100-nm-thick MgAg cathode layer (Mg/Ag = 10/1 by weight) was thermally evaporated in a vacuum on the Alq_3 layer to complete the devices. The *J*-*V* characteristics of the devices were obtained using a semiconductor parameter analyzer (E5250A, Agilent Technology Co.) at room temperature. In this work, we assumed that HOMO and lowest unoccupied molecular orbital (LUMO) levels of the evaporated organic thin films are identical with their ionization potential energies and electron affinities, respectively. To depict the energy-band diagram shown in Fig.1, the work functions of the ITO and

MgAg electrodes and the ionization potential energies of the organic thin films were measured by ultraviolet photoelectron spectroscopy (AC-1, Rikenkeiki Co.), and the electron affinities of the organic thin films were calculated by subtracting their optical absorption onset energies (energy gap) from the ionization potential energies.

The chemical structures of all organic materials and the energy-band diagram of the devices are shown in Fig. 1. We used 24 kinds of guest molecules with HOMO levels that were systematically varied between -4.7 and -6.7 eV. Although phthalocyanine derivatives such as NiPc, ZnPc, CuPc, CoPc, and PbPc exhibit no EL in the visible region, we used these materials to obtain their *J*-*V* characteristics. These systematic variations of the HOMO levels provided us with important insights for clarifying current flow mechanisms of the OLEDs.

Figure 2 shows the *J*-*V* characteristics of the devices doped with the various guest molecules. The *J*-*V* characteristics shifted to higher current densities when increasing the HOMO levels of the guest molecules from -4.7 to -5.3 eV, and the *J*-*V* characteristics of the device doped with the AC-5 guest molecule having the HOMO level of -5.3 eV exhibited the highest current density among the devices [Fig. 2(a)]. Reversely, the *J*-*V* characteristics shifted to lower current densities when increasing the HOMO levels of the guest molecules from -5.3 to -6.0 eV [Fig. 2(b)]. These results

indicate that the *J-V* characteristics are controlled by direct hole injection from the TPD to guest molecules, i.e., the hole injection at this interface is the rate-limiting process of the *J-V* characteristics. Moreover, the *J-V* characteristics were almost unchanged for the devices doped with the guest molecules having the HOMO levels ranging from -6.0 to -6.7 eV [Fig. 2(c)]. In this case, since the heights of the energy barriers between the TPD and guest molecules are relatively large (0.7-1.4 eV), most holes are predominantly injected from the TPD to CBP molecules instead of the guest molecules, resulting in the unchanged *J-V* characteristics.

Figure 3 shows the plots of the LUMO and HOMO levels of the guest molecules versus the current densities obtained from the devices operated at a driving voltage of 10 V. Although we observed no clear relationship between the current densities and the LUMO levels [Fig. 3(a)], the HOMO-current density characteristics showed the convex curve as shown in Fig. 3(b). The highest current density was obtained at the HOMO level of -5.3 eV, which is identical with that of the TPD HTL. Therefore, we conclude that HOMO level alignment between the TPD and guest molecules provides efficient hole injection at this interface.

Figure 4 illustrates hole injection processes at the TPD/CBP interfaces. Carrier transport in amorphous organic thin films occurs through positionally random and

energetically disordered carrier-hopping states within the localized density-of-states (DOS) distributions [10-12]. Therefore, the overlap areas of two DOS distributions markedly influence carrier injection efficiencies at organic/organic heterojunction interfaces. The hole injection processes of our devices can be classified into three types: across downward energy barriers [Fig. 4(a)], without energy barriers [Fig. 4(b)], and across upward energy barriers [Figs. 4(c), 4(d), and 4(e)]. Although the processes in (a) and (b) are generally advantageous for hole injection, in our devices we observed that both upward and downward energy barriers lowered hole injection efficiencies. As the HOMO levels of the guest molecules were increased from -4.7 to -5.3 eV, the heights of the downward energy barriers between the TPD and guest molecules decreased, leading to a gradual increase in hole injection efficiency and current density [region (I) in Figs. 3(b) and 4(a)]. When the HOMO level of the guest molecule was aligned to that of the TPD layer, the device reached the highest hole injection efficiency and current density [region (II) in Figs. 3(b) and 4(b)]. In contrast, increasing the HOMO levels of the guest molecules from -5.3 to -6.0 eV induced a gradual increase in the heights of the upward energy barriers, again leading to a decrease in hole injection efficiency and current density [region (III) in Figs. 3(b) and 4(c)]. In the HOMO level region between -6.0 and -6.7 eV, the observed current densities were constant. We can divide this region in two

parts, regions (IV) and (V) [see Fig 3(b)]. In the region (IV), holes are mainly injected from the TPD to CBP molecules and partly injected from the TPD to guest molecules [Fig. 4(d)] because there are relatively high energy barriers ranging from 0.7 to 1.0 eV at the TPD/guest heterojunction interfaces and the guest concentration is only 5 mol% relative to the CBP host molecules. In the region (V), all holes are injected in the CBP layer because the HOMO levels of the guest molecules are deeper than those of the CBP molecules [Fig. 4(e)]. Such hole injection in the CBP molecules makes the *J*-*V* characteristics similar to the non-doped devices.

We demonstrated that doping guest molecules in CBP host matrix layers markedly influenced *J*-*V* characteristics in OLEDs. In our devices, we found that *J*-*V* characteristics were mainly controlled by direct hole injection from a TPD HTL to guest molecules. When the HOMO level of a guest molecule was aligned to that of the TPD hole-transporting layer (-5.3 eV), a device reached the highest hole injection efficiency and current density due to the largest overlap area of DOS distributions of the TPD and guest molecules, while devices doped with guest molecules having HOMO levels other than -5.3 eV showed lower current densities.

Acknowledgements

The authors thank Dr. Seiji Akiyama (*Optoelectronic Materials Laboratory, Research and Technology Development Division, Mitsubishi Chemical Group, Science and Technology Research Center, Inc*.) and Hiroyuki Uchiuzou (*Department of Photonics Materials Science, Chitose Institute of Science and Technology*) for synthesizing and purifying organic materials used in this experiment such as BPSB, TBPPY, F-TPPY, F_2-TPPY, and TBPNA.

References

[1] C. W. Tang, S. A. Van Slyke, C. H. Chen, J. Appl. Phys. 65 (1989) 3610.

[2] K. Okumoto, H. Kanno, Y. Hamaa, H. Takahashi, K. Shibata, Appl. Phys. Lett. 89 (2006) 063504.

[3] C. Adachi, M. A. Baldo, S. R. Forrest, M. E. Thompson, Appl. Phys. Lett. 77 (2000) 904.

[4] C. Adachi, M. A. Baldo, M. E. Thompson, S. R. Forrest, J. Appl. Phys. 90 (2001) 5048.

[5] M. Ikai, S. Tokito, Y. Sakamoto, T. Suzuki, Y. Taga, Appl. Phys. Lett. 79 (2001) 156.

[6] G. He, M. Pfeiffer, K. Leo, M. Hofmann, J. Brinstock, R. Pudzich, J. Salbeck, Appl. Phys. Lett. 85 (2004) 3911.

[7] C. Adachi, T. Tsutsui, S. Saito, Appl. Phys. Lett. 57 (1990) 531.

[8] C. Adachi, M. A. Baldo, S. R. Forrest, J. Appl. Phys. 87 (2000) 8049.

[9] C.-H. Cheng, Z.-Q. Fan, S.-K. Yu, W.-H. Jiang, X. Wang, G.-T. Du, Y.-C. Chang, C.-Y. Ma, Appl. Phys. Lett. 88 (2006) 213505.

[10] V. I. Arkhipov, U. Wolf, H. Bässler, Phys. Rev. B 59 (1999) 7514.

[11] V. I. Arkhipov, E. V. Emelianova, H. Bässler, J. Appl. Phys. 90 (2001) 2352.

[12] V. R. Nikitenko, O. V. Salata, H. Bässler, J. Appl. Phys. 92 (2002) 2359.

Figure Captions

Fig. 1. Chemical structures of organic materials and energy-band diagram of devices doped with various guest molecules. Guest material was doped in CBP matrix layer at doping concentration of 5 mol%.

Fig. 2. Current density-voltage (*J*-*V*) characteristics of devices doped with various guest molecules. HOMO levels of guest molecules are varied between (a) -4.7 and -5.3 eV, (b) -5.3 and -6.0 eV, and (c) -6.0 and -6.7 eV.

Fig. 3. Plots of (a) LUMO and (b) HOMO levels of guest molecules versus current densities of devices operated at driving voltage of 10V.

Fig. 4. Schematic illustrations of hole injection processes at TPD/guest-doped CBP interfaces, (a) direct hole injection across downward energy barrier from TPD to guest molecules, (b) direct hole injection without energy barrier from TPD to guest molecules, (c) direct hole injection across upward energy barrier from TPD to guest molecules, (d) hole injection across upward energy barrier from TPD to both CBP and guest molecules, and (e) hole injection across upward energy barrier from TPD to CBP molecules.

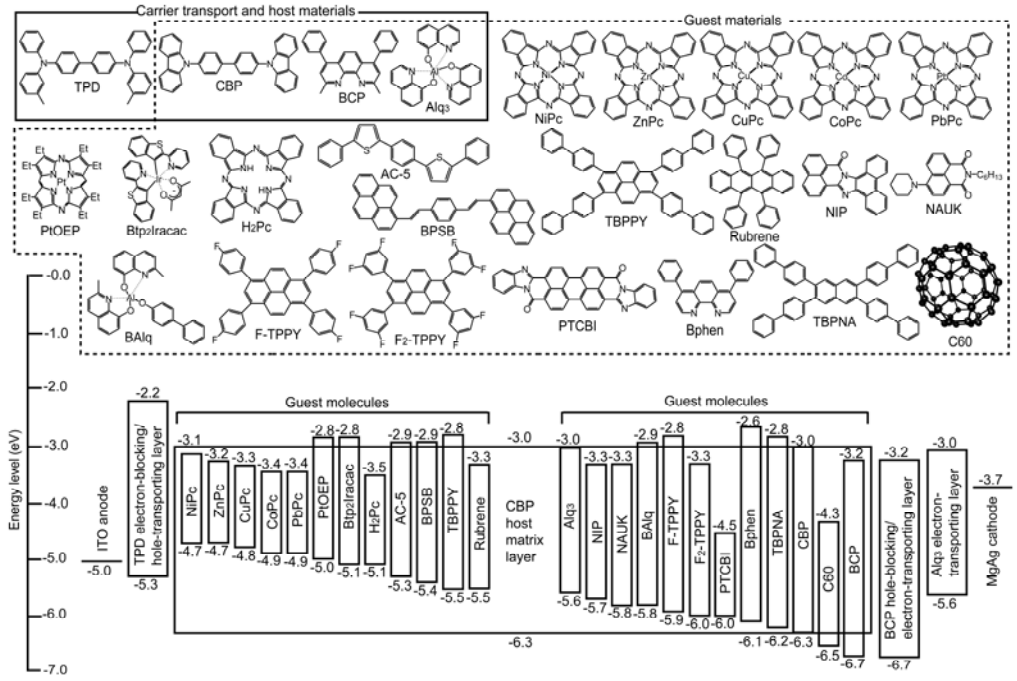

Fig. 1. T. Matsushima *et al*.
Chemical Physics Letters

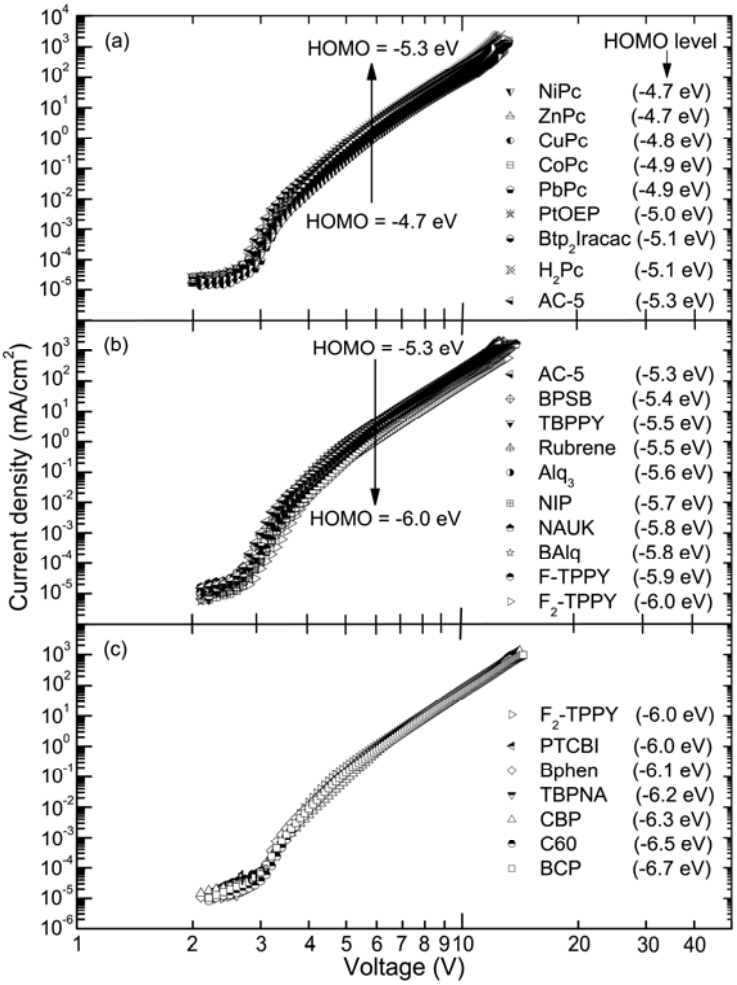

Fig. 2. T. Matsushima *et al*.
Chemical Physics Letters

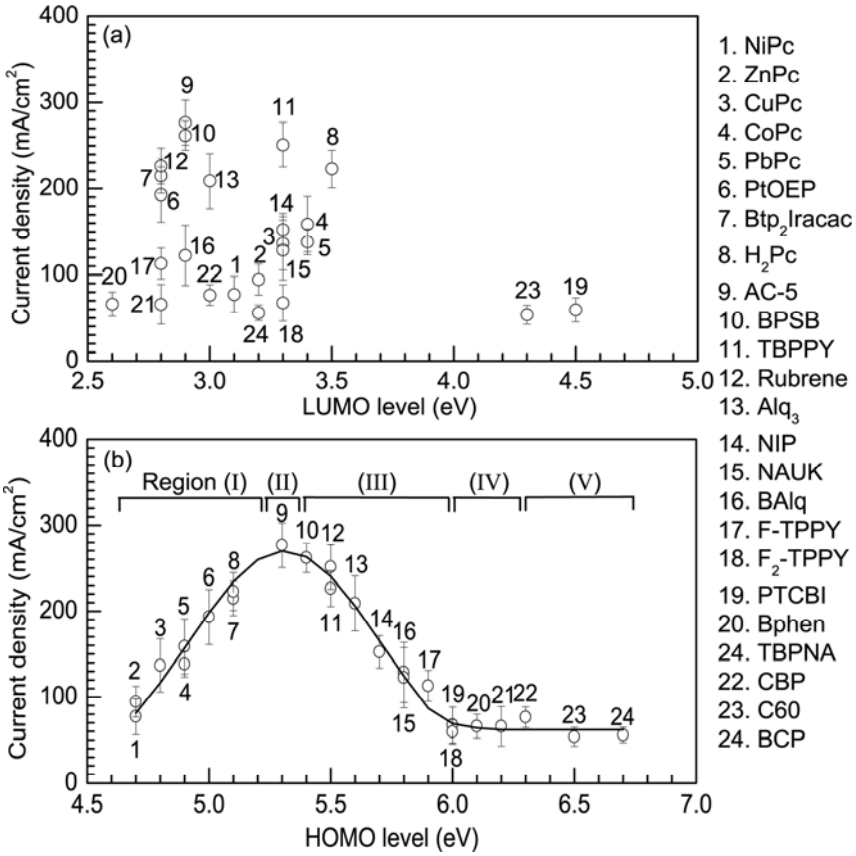

Fig. 3. T. Matsushima *et al*.
Chemical Physics Letters

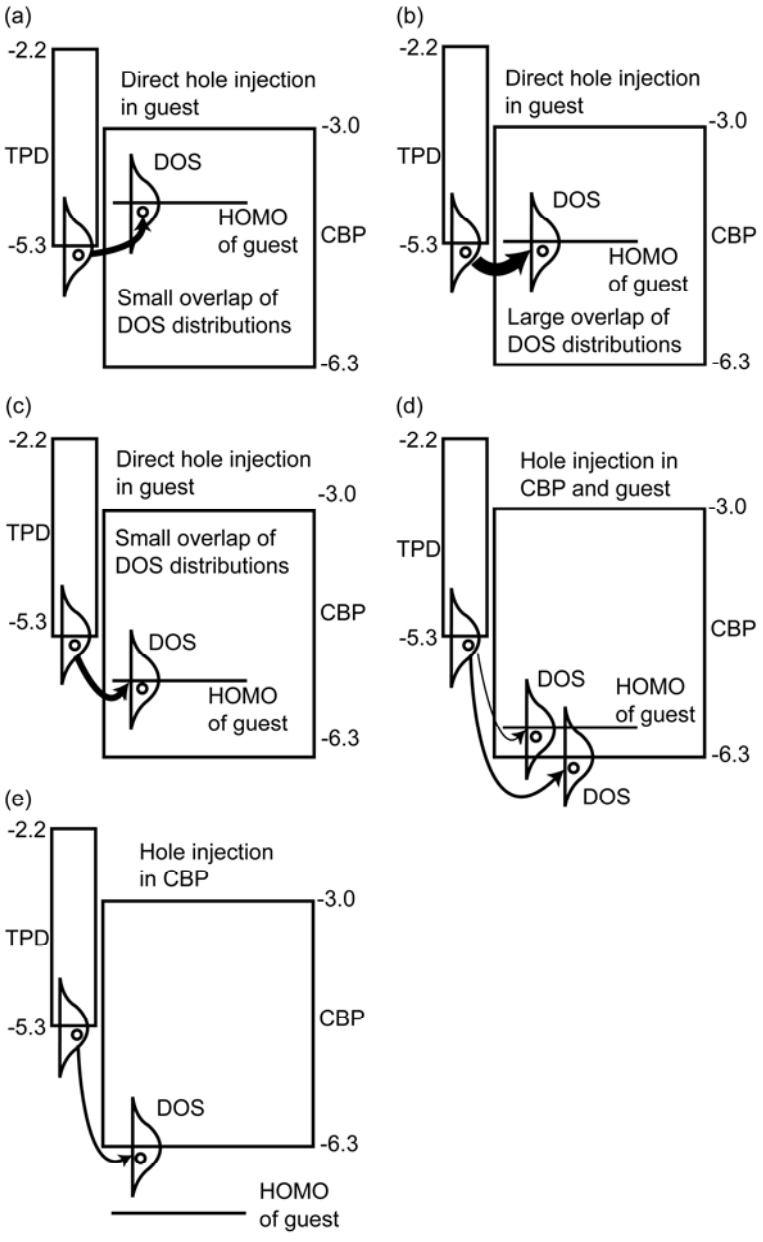

Fig. 4. T. Matsushima *et al*.
Chemical Physics Letters